From Wet Gel to the Final Product: Draw Your Way

Chapter 4
From wet gel to the final product: draw your way

Abstract

Once the gel is obtained, the water and alcohol that fill the porosity of the solid network must be removed through drying treatments to readily convert the wet gel in a dry solid. The methods of liquid extraction, as well as the other steps in the sol-gel process, can play an important role in determining the surface properties of the final material. Moreover, the combination of the drying procedure and the protocol to be adopted can be a decisive factor in yielding a highly porous material. In most cases, wet gels are dried in an oven at a temperature of around 100 °C to produce so-called xerogels. The difference in the contraction speed between inside and outside the gel is responsible for the formation of cracks. Outstanding and somewhat unusual properties can be achieved if the gels are dried by supercritical drying, resulting in what are called aerogels. In particular, aerogels are characterised by very low apparent densities, large specific surface areas and, in most cases, have amorphous structures. In more recent times, other drying methods have become popular that allow for high pore interconnection and large surface to volume ratio, usually between xerogel and aerogel. These include the freeze-drying process from which cryogels are obtained.

Keywords: wet gel, drying, xerogel, aerogel, cryogel, film formation

4.1 Drying methods

During classic stove drying, under constant temperature, pressure and humidity conditions, the water and alcohol trapped in the gel matrix are removed in a process driven by capillary tension, which, if not properly controlled, leads to a simultaneous collapse of the gel structure, Figure 4.1.

In the first step of this process, the gel structure is compliant and responds to the increase in capillary tension with a gradual shrinkage, leaving liquid-vapor interface at the exterior gel surface [1,2]. The reduction in volume is simultaneously accompanied by further cross-linking of the lattice due to the approaching of condensable groups and the formation of new siloxane bonds. This phenomenon leads to a stiffening of the gel, which begins to resist further contraction until it reaches a critical point where stress is at its highest. It is at this point that the textural properties of the dry product, called xerogel, are defined. In order to prevent fracture formation, the rigidity of the gel must be increased, providing resistance to collapse, and the capillary pressure that causes the gel to collapse must be limited. Slow drying certainly causes a more uniform compression of the lattice, decreasing the tendency to fracture, but it would increase the xerogel formation time, negatively affecting the entire process.

The average pore size formed during the drying process contributes largely to the effectiveness of solvent removal while the strength of the gel helps to contrast capillary tension.

Careful control of the molar ratios of alkoxide/water/alcohol and the type of catalysis can be a means of achieving pore enlargement and network strengthening [1,3]. A more innovative strategy for crack-free gels is the adoption of a surfactant as a model for the uniform pore network. This decreases the capillary tension gradient in the gel, which is the real factor causing the formation of cracks [4].

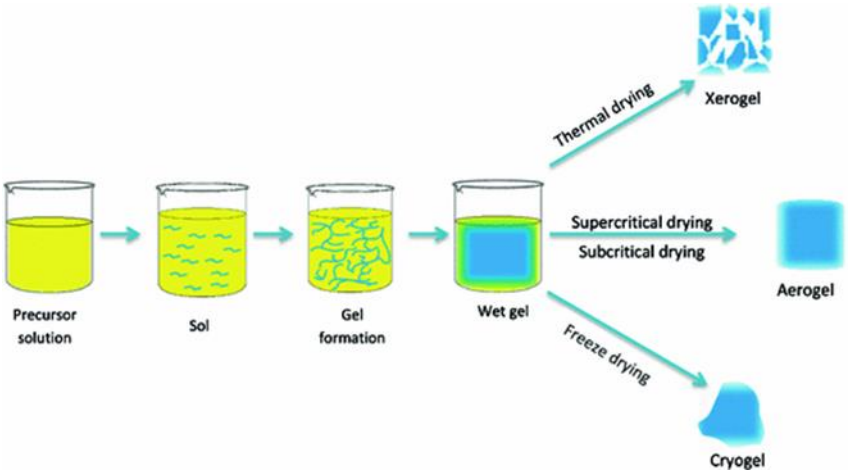

Figure 4.1 Schematic representation of wet gel formation and possible drying procedures. Adapted with permission from [2] Copyright 2017 Springer

Another strategy to circumvent gel collapse involves drying under supercritical conditions, a more sophisticated procedure that removes the obstacle of the capillary pressure gradient by working at a pressure and temperature higher than those corresponding to the critical point of a liquid trapped in the gel pores, Figure 4.1.

After replacing the water with a specific solvent, the system is brought to supercritical fluid conditions, at this point the pressure and temperature are gradually released, allowing the gas to escape and leaving a dried product. Among possible supercritical solvents, carbon dioxide has the advantage of less drastic conditions, in particular the critical temperature is close to the room temperature: 31 °C and 7.4 MPa (for ethanol it is 243 °C and 6.4 MPa).

Aerogels possess outstanding physical properties, such as very low thermal conductivity, high temperature resistance, and good mechanical properties combined with very low density, the pore volume is above 90% of the sample volume. The name aerogel does not refer to a specific chemical composition but, rather, to this unique structure composed essentially of air. The most prominent features that have aroused the interest of researchers working in the field of catalysis are the very high porosity, high specific surface areas and the possibility of modelling the material [5,6]. Although the industry is dominated by silica aerogels and their use as composite blankets in energy and industrial insulation, the strong impetus from scientific research is broadening the fields of application of aerogel. Indeed, a wide range of substances prepared in the form of aerogels are used in optical, electrical, environmental, biomedical and catalytic applications [7-12].

The lack of an effective boom in the aerogel industry is largely linked to the fragility of these materials, which limits their commercial use as part of a composite design, and the need to reduce the cost of the supercritical drying process. For this reason, improvements to supercritical drying continue to be sought along with the development of alternative processes, including ambient pressure drying and freeze-drying.

Freeze-drying, also known as Lyophilisation or cryo-drying, is a slow process that removes water or other solvents from frozen samples through sublimation and desorption under vacuum, Figure 4.1. The final porous architecture, benefiting from the 'ice crystal model effect', is represented by highly interconnected macroporous structures [13,14]. Toshihiko Osaki [15] showed how the freeze-drying process can be a strategy to impact the structural and textural properties of catalysts.

Ni/Al_2O_3 cryogel was synthesised from aluminium sec-butoxide and nickel acetate by a one-pot sol-gel process followed by lyophilisation. Comparison with an analogous Ni/Al_2O_3 xerogel gel revealed the characteristics of the cryogel that led to higher performance in reforming CH_4 from CO_2. In particular, an increase in surface area and pore volume was observed, figure 4.2. It was also found that the average nickel particle size for cryogel was about 87% of that of xerogel, thus limiting carbon formation, figure 4.2 [15].

a

Table 1 BET surface area (*BET-SA*), pore volume (V_p), peak pore radius (R_p), crystallite size of nickel (D_{hkl}), volume-area mean diameter of nickel (d_{VA}), and CO chemisorption number

Catalyst	*BET-SA*		V_p		R_p		D_{hkl}	d_{VA}	CO adsorption
	$m^2 g^{-1}$		$mm^3 g^{-1}$		nm				
	Calcination[a]	Reduction[b]	Calcination[a]	Reduction[b]	Calcination[a]	Reduction[b]	nm	nm	μmol g^{-1}
Cryogel	283	205	350	309	2.1	3.0	2.5	4.8	105
Xerogel	241	161	275	260	2.1	3.2	4.6	5.5	109
Imp(cryo)	230	190	348	315	3.2	3.0	6.9	7.4	114
Imp(com)	142	125	399	487	5.1	6.1	10.5	10.5	103

[a]At 500 °C for 1 h

[b]At 800 °C for 1 h

b

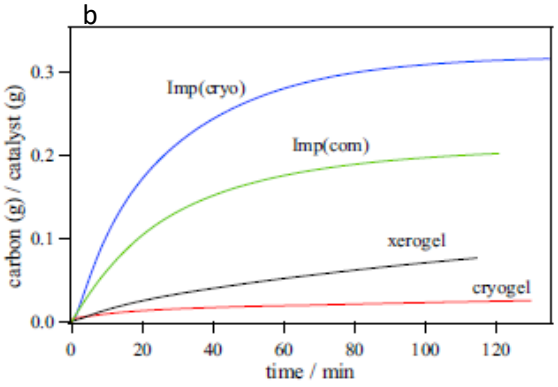

Figure 4.2 Textural properties of Ni/Al_2O_3 gel (a) and TG profiles of carbon formation on the catalysts under CH_4–CO_2 atmosphere at 800 °C (b). Adapted with permission from [15] Copyright 2021 Springer

4.2 Thin film formation

The drying of the gel can be forced if the surface area in contact with the atmosphere is increased, which is what happens in the production of thin films. The preparation of thin films, using dip-coating or spin-coating techniques, is indeed one of the most important and intriguing applications of sol-gel processing. While from the point of view of instrumentation, film deposition can be considered a rather simple procedure, from the point of view of the chemistry of the solution, adhesion to the substrate and the formation of the film itself, the process can be challenging.

In the preparation of thin films, the drying stage overlaps with the aggregation/gelation and ageing steps. Consequently, the formation of a crack-free film, as well as its final structure, are the consequence of competitive phenomena such as evaporation (which compacts the film), condensation reactions (which strengthen the film, increasing its resistance to compaction) and shear-induced ordering [16].

The 'sol' that meets the requirements for film deposition must be stable and of adequate viscosity. As mentioned in previous chapters, throughout the gel formation, viscosity increases very slowly, then undergoes a sudden exponential increase followed by instantaneous gelling.

It is therefore crucial to monitor the parameters affecting the polymerisation kinetics of metal alkoxide, in order to have a sol with a high degree of hydrolysis and adequate viscosity. But, at the same time, the factors that rule the film deposition process on the substrate can be decisive in obtaining a uniform crack-free film [17-19].

A successful attempt to prepare humidity-sensitive $CoOx\text{-}SiO_2$ thin films in a reasonable time scale was realised by Esposito et al. [18]. The strategy adopted was to hydrolyse TEOS under acidic conditions in the absence of alcohol, resulting in a sol with a high degree of cross-linking after 2 days. Moreover, the absence of alcohol makes easier to solubilise an high amount of inorganic salt precursors, up to 30 mol%. To achieve the appropriate viscosity for the deposition of a uniform crack-free film, the solution was subsequently diluted with anhydrous ethanol. Silica glass slides were dipped into the solution and withdrawn at a speed of 100 mm min^{-1}. Transparent pinkish films were obtained that were fully dried and then annealed at different temperatures in the range 400-1000 °C, Figure 4.3. Film thickness was estimated to be approximately 0.8 ± 0.03 μm [18].

One of the advantages of the sol-gel method over conventional coating methods such as sputtering/evaporation and CVD (chemical vapor deposition) is the possibility to control the microstructure of the film (pore volume, pore size and surface area) [20].

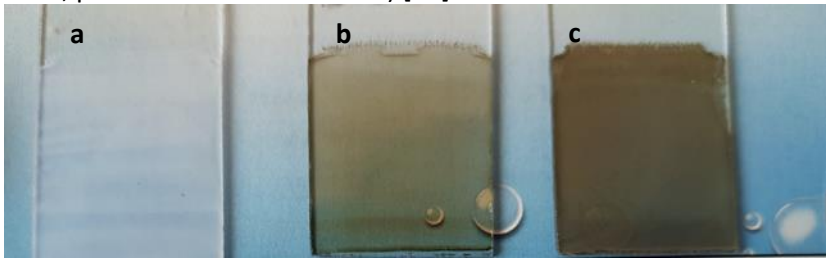

Figure 4.3 CoOx-SiO_2 thin films prepared by dip coating and heat treated at a) 1000 °C; b) 300 °C and c) 400 °C.

The microstructures of thin films obtained by dipping and spinning are largely dependent on process parameters such as withdrawal rate, spinning speed, surface tension, viscosity and evaporation rate.
The dip coating process can be seen as the sum of several steps, Figure 4.4.
First, the substrate is immersed in the sol at a constant rate and for a period of time sufficient to ensure the interaction of the substrate with the film precursors.
In a next step, the substrate is pulled upwards at a constant speed. If the sol has the right viscosity characteristics and the right degree of cross-linking, the substrate drags the solution towards the deposition region. The adhesion to the substrate that ensures subsequent film formation is a competition between the viscous drag that holds the fluid on the substrate and the gravity force that moves the fluid away from the substrate [16].
The extraction of the substrate from solution causes a rapid increase in the liquid-vapour separation surface, triggering rapid evaporation of the volatile components. The resulting increase in the concentration of the reagents in the forming film compared to the concentration in solution strongly fosters polycondensation reactions leading to almost instantaneous gelation. The obtained coating undergoes further heat treatment, which burns off residual organics and induces crystallisation of the functional oxides. The heating stage can be remarkably critical in the formation of cracks and unavoidable peeling off of local areas. Indeed, fractures are assumed to be caused by stress resulting from the deformation introduced by the condensation of the silanol groups and the evaporation of the residual organic substances [21-22].

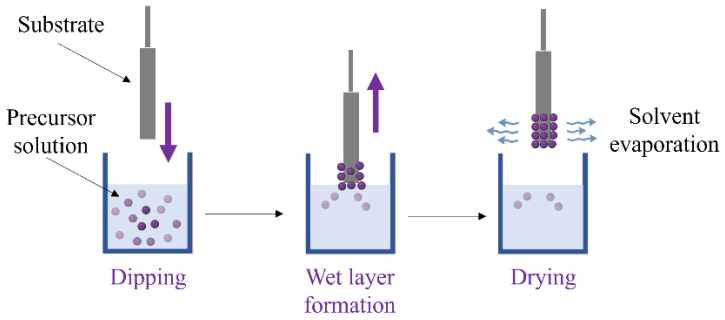

Figure 4.4 A schematic view of the dip-coating method

The thickness of the film is related to the processing parameters and can reasonably calculated from eq. 1 derived from Landau and Levich model [23].
According to this model, the thickness of the film is proportional to the viscosity of the colloidal solution and the extraction rate, and inversely proportional to the liquid vapor surface tension according to the following equation

$$h = 0.94 \frac{\eta v^{2/3}}{\gamma^{1/6} (\rho g)^{1/2}} \quad (1)$$

In this equation, η is the viscosity of the solution, v is the withdrawal speed from the solution, ρ is the density of the solution, g is the gravity acceleration and γ is the liquid-vapour surface tension.
In addition to all the parameters that have been mentioned, the roughness of the support and its chemical affinity with the film can affect the formation of a uniform coating and its final thickness [23].
The strategy, used by Emiel J. Kappert et al. [24], to prevent crack tendency in silica films was to replace part of the TEOS with an alkyl-substituted silane. Although the synthesis was designed to retain the same microstructure for silica and organosilica, the results obtained show that organosilica materials have much larger critical thicknesses than silica [24].

The spin coating method overcomes some of the limitations of dip coating, such as double side coating and non-uniformity at the wafer edge. In the spin-coating method, the sol is dripped onto the substrate in an adequate quantity to subsequently cover the entire surface. When the substrate is spun at a predetermined speed, the liquid flows radially outwards due to the centrifugal force. As the film thins, the speed at which the excess liquid is removed slows down. The deposited film assumes uniform thickness as a result of balancing action between two types of forces, i.e. centrifugal force and viscous (friction) force [25].

Promising new fields for nanostructured oxides, which include photocatalysis and electrocatalysis, require their processing as mesostructured thin films [26,27].

The Evaporation Induced Self-Assembly Method, EISA, was first reported by Osawa and Brinker [28-30] to prepare mesoporous silica thin film. The technique is based on the same principle as mesostructured silicas, that is the ability of surfactants to self-assemble into various structures. However, in the deposition of mesoporous thin film, the self-assembly is driven by the evaporation of the solvent during the withdrawal of the support from the solution, Figure 4.5 [31, 32].

The process of forming mesoporous thin films using EISA begins with the preparation of a dilute solution containing mainly inorganic (or hybrid) precursors, solvents, catalysts and a surfactant, Figure 4.5.

When the substrate is extracted from the solution, rapid evaporation of the solvent occurs and the concentrations of the metal oxide oligomers and the non-volatile surfactant increase. When the surfactant concentration is equal to the critical micelle concentration, cmc, micelles form and an organised Liquid Crystal (LC) mesophase is obtained while the inorganic network is not completely condensed. In this stage of film formation, the relative humidity (RH) conditions play a key role. In the final stage, the template is removed to impart porosity and completely condense the inorganic network [33].

A big advantage of the EISA process when combined with dip-coating is the flexibility afforded in controlling the final mesostructure of the thin film by careful control of processing parameters such as temperature, time, RH, vapor pressure and chemical parameters such as composition and pH.

The preparation of reproducible mesoporous thin films requires understanding and control at three main levels: the chemistry associated with the initial solution, the processes linked to the layer deposition technique and the treatment aimed at eliminating the organic phase and stiffening the network without pore collapse [34].

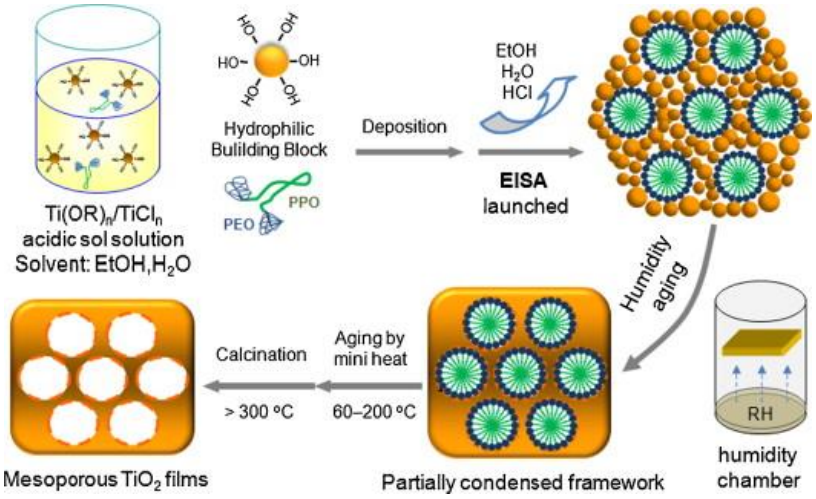

Figure 4.5 Schematic representation of EISA process for the synthesis of highly organized mesoporous TiO_2 films. Adapted with permission from [32]; Copyright 2011 Elsevier

References

1. F. Kirkbir, H. Murata, D. Meyers, S. RAY Chaudhuri, A. Sarkar, Drying and Sintering of Sol-Gel Derived Large SiO2 Monoliths. J. Sol-Gel Sci. Technol. 1996, 6, 203-217.
2. S. Dervin, S.C. Pillai, (2017). An Introduction to Sol-Gel Processing for Aerogels. In: Pillai, S., Hehir, S. (eds) Sol-Gel Materials for Energy, Environment and Electronic Applications. Advances in Sol-Gel Derived Materials and Technologies. Springer, Cham. https://doi.org/10.1007/978-3-319-50144-4_1
3. A. Fidalgo, M. E. Rosa, L. M. Ilharco, Chemical Control of Highly Porous Silica Xerogels: Physical Properties and Morphology. Chem. Mater. 2003, 15 (11), 2186–2192.
4. M.J. Mosquera, D.M. de los Santos, L. Valdez-Castro, L. Esquivias, New route for producing crack-free xerogels: Obtaining uniform pore size. J. Non-Cryst. Solids 2008, 354, 645–650.
5. T. Wu, M. Chen, L. Zhang, X. Xu, Y. Liu, J. Yan, et al. Three-dimensional graphene-based aerogels prepared by a self-assembly process and its excellent catalytic and absorbing performance. J Mater Chem A. 2013, 1, 7612–21.
6. Z. Zhou, X. Zhang, C. Lu, L. Lan, G. Yuan Polyaniline-decorated cellulose aerogel nanocomposite with strong interfacial adhesion and enhanced photocatalytic activity. RSC Adv. 2014, 4, 8966–72.
7. A.C. Pierre, and G.M. Pajonk, Chemistry of Aerogels and Their Applications. Chem. Rev. 2002, 102, 4243-4265.
8. J. Choi, D. J. Suh, Catalytic Applications of Aerogels. Catalysis Surveys from Asia 2007, 11, 123–133.
9. Y. Guo, C. Zhao, J. Sun, W. Li, P. Lu Facile synthesis of silica aerogel supported K2CO3 sorbents with enhanced CO_2 capture capacity for ultra-dilute flue gas treatment. Fuel. 2018, 215, 735–43.
10. Z. Ali, A. Khan, R. Ahmad, The use of functionalized aerogels as a low-level chromium scavenger. Microporous Mesoporous Mater. 2015, 203, 8–16;
11. S. Zhao, B. Jiang, T. Maeder, P. Muralt, N. Kim, S.K. Matam, et al. Dimensional and structural control of silica aerogel membranes for miniaturized motionless gas pumps. ACS Appl Mater Interfaces. 2015, 7, 18803–14;
12. Hamann TW, Martinson AB, Elam JW, Pellin MJ, Hupp JT. Atomic layer deposition of TiO2 on aerogel templates: new photoanodes for dye sensitized solar cells. J Phys Chem C. 2008, 112, 10303–10307.
13. X. Wang, A. Sumboja, E. Khoo, C. Yan, P.S. Lee, Cryogel Synthesis of Hierarchical Interconnected Macro-/Mesoporous Co_3O_4 with Superb Electrochemical Energy Storage. J. Phys. Chem. C 2012, 116, 4930−4935.
14. L. B. Chiriac, M. Todea, A. Vulpoi, M. Muresan-Pop, R. V. F. Turcu, S. Simon. Freeze-drying assisted sol–gel-derived silica-based particles embedding iron: synthesis and characterization. Journal of Sol-Gel Science and Technology 2018, 87, 195–203.
15. T. Osaki, Synthesis of porous and homogeneous Ni/Al2O3 cryogel for CO2 reforming of CH4. J Sol-Gel Sci Technol 2021, 97, 291-301.
16. C.J. Brinker, A.J. Hurd, G.C. Frye, K.J. Ward and C.S. Ashley, Sol-Gel thin film formation. Journal of Non-Crystalline Solids 1990, 121, 294-302.
17. M. D'Apuzzo, A. Aronne, S. Esposito, P. Pernice, Sol-Gel Synthesis of Humidity-Sensitive P2O5-SiO2 Amorphous Films. J. Sol-Gel Sci. Technol. 2000, 17, 247–254.
18. S. Esposito, A. Setaro, P. Maddalena, A. Aronne, P. Pernice, M. Laracca, Synthesis of cobalt doped silica thin film for low temperature optical gas sensor. J Sol-Gel Sci. Technol. 2011, 60, 388–394
19. G. Dell'Agli, S. Esposito, G. Mascolo, M.C. Mascolo, C. Pagliuca, Films by slurry coating of nanometric YSZ (8 mol% Y_2O_3) powders synthesized by low-temperature hydrothermal treatment. Journal of the European Ceramic Society 2005, 25, 2017–2021.
20. K. Haas-Santo, M. Fichtner, K. Schubert, Preparation of microstructure compatible porous supports by sol–gel synthesis for catalyst coatings. Applied Catalysis A: General 2001, 220 (1-2), 79-92.
21. Sumio Sakka in Handbook of Advanced Ceramics: Chapter 11.1.2. Sol–Gel Process and Applications. Materials, Applications, Processing, and Properties, Book, Second Edition 2013 Academic Press, Editor in chief Shigeyuki Somiya. 10.1016/B978-0-12-385469-8.01001-7.
22. T.J. Garino, The Cracking of Sol-Gel Films During Drying. MRS Online Proceedings Library 1990, 180, Article number: 497.

23. J.P. Fernández-Hernán, A.J. López, B. Torres, J. Rams, Influence of roughness and grinding direction on the thickness and adhesion of sol-gel coatings deposited by dip-coating on AZ31 magnesium substrates. A Landau–Levich equation revision. Surface & Coatings Technology 2021, 408, 126798.
24. E.J. Kappert, D. Pavlenko, J. Malzbender, A. Nijmeijer, N. E. Benes, P. A. Tsaj, Formation and prevention of fractures in sol–gelderived thin films. Soft Matter, 2015, 11, 882-888.
25. K. Vorotilov, V. Petrovsky, V. Vasiljev, Spin Coating Process of Sol-Gel Silicate Films Deposition: Effect of Spin Speed and Processing Temperature. J. Sol-Gel Sci. Technol. 1995, 5, 173-183.
26. M. Einert, M. Mellin, N. Bahadorani, C. Dietz, S. Lauterbach, Jan P. Hofmann, Mesoporous High-Entropy Oxide Thin Films: Electrocatalytic Water Oxidation on High-Surface-Area Spinel $(Cr_{0.2}Mn_{0.2}Fe_{0.2}Co_{0.2}Ni_{0.2})_3O_4$ Electrodes. ACS Appl. Energy Mater. 2022, 5, 1, 717–730.
27. W. Zhou, W. Li, Q.J. Wang, Y. Qu, Y. Yang, Y. Xie, K. Zhang, L. Wang, H. Fu, D. Zhao, Ordered mesoporous black TiO_2 as highly efficient hydrogen evolution photocatalyst. J. Am. Chem. Soc. 2014, 136, 9280–9283.
28. M. Ogawa, Preparation of Layered Silica−Dialkyldimethylammonium Bromide Nanocomposites. Langmuir 1997, 13, 1853-1855.
29. C. J. Brinker, Y. F. Lu, A. Sellinger, H. Y. Fan, Evaporation-Induced Self-Assembly: Nanostructures Made Easy. Adv. Mater. 1999, 11, 579-585.
30. C. J. Brinker, Evaporation-Induced Self-Assembly: Functional Nanostructures Made Easy. MRS Bull. 2004, 29, 631-640.
31. T. Brezesinski, M. Groenewolt, A. Gibaud, N. Pinna, M. Antonietti, B.M. Smarsly, Evaporation-Induced Self-Assembly (EISA) at Its Limit: Ultrathin, Crystalline Patterns by Templating of Micellar Monolayers. Adv. Mater. 2006, 18, 2260–2263.
32. J.H. Pan, X.S. Zhao, W.I. Lee, Block copolymer-templated synthesis of highly organized mesoporous TiO_2-based films and their photoelectrochemical applications. Chem. Eng. J. 170 (2011) 363–380.
33. L. Mahoney, R. T. Koodali, Versatility of Evaporation-Induced Self-Assembly (EISA) Method for Preparation of Mesoporous TiO_2 for Energy and Environmental Applications. Materials 2014, 7, 2697-2746; doi:10.3390/ma7042697.
34. C.J. Brinker, R. Sehgal, S.L. Hietala, R. Deshpande, D.M. Smith, D. Loy and C.S. Ashley, Sol-gel strategies for controlled porosity inorganic materials. Journal of Membrane Science 1994, 94, 85-102.